

Some New Results on Momentum and Heat Transfer in Compressible Turbulent Free Jets

JOHN F. TOMICH and ERIC WEGER

Washington University, St. Louis, Missouri

The results of an analytical and experimental study of compressible, axially symmetric, turbulent free jets exhausting into quiescent air are presented. A finite-difference technique was used to obtain a general solution which has eliminated the need for the simplifying assumptions required in previous investigations. The jet Mach number and jet temperature ratio have been found to be the only two initial jet properties which are necessary to characterize the dimensionless velocity and temperature variations in this type of jet. Modifications of dynamic eddy transfer coefficients given in the literature are used in the solution. An experimental program was carried out to obtain data on free jet velocity and temperature variation at high initial jet temperatures and high subsonic Mach numbers where there has been a lack of experimental data. The numerical solutions of the time-averaged conservation equations have been shown to agree well with the experimental data of the present study and of previous investigations.

The frequent use of compressible, turbulent gas jets in modern aerospace, chemical, and mechanical technology has led to a need for information which will permit more accurate prediction of the temperature and velocity fields in these jets. This paper reports the results of numerical calculations and experimental studies that extend the presently available methods of describing free jet characteristics.

The structure of the compressible, axially symmetric free jet can be described in terms of three flow regions (Figure 1). The potential core region extends to the point where the turbulent mixing region reaches the jet axis. This region is, of course, not necessarily identical for velocity and temperature. The next region is a transition region where the spread of the jet in the radial direction and the axial decay of the center line properties are very rapid. This is followed by the fully developed region where the radial spread of the jet is nearly linear with respect to axial distance. The greater the compressible effects, the greater is the deviation from linearity.

There are many problems which arise in connection with any numerical approach to the problem of solving for temperature and velocity as a function of position in the compressible jet. One is the nonexistence of similarity (1) in the profiles (as distinct from the case for incompressible flow). The model must also take into account the fact that the jet only becomes fully developed a certain number of nozzle diameters downstream from the nozzle. Therefore a complete treatment must include the potential core region and the transition region, as well as the fully developed portion of the jet. The boundary conditions also are a source of difficulty. These include the prescribed conditions at the nozzle (that is, flat or other types of profiles) and the conditions at an

infinite radial distance (that is, whether the jet is exhausting into a moving gas stream or into quiescent surroundings).

Because of these problems, most of the available calculational techniques had to employ various simplifying assumptions that limited their usefulness. Much of the work has been restricted to the problem of axial velocity and temperature decay, while the question of the radial variation of these quantities has not been dealt with extensively. Another limitation in previous work has been that even when nonisothermal systems were being studied, the range of temperatures used in experimental studies was usually too small to bring out variations in the eddy transfer coefficients with density. It was the intent of the present study to overcome some of these limitations.

Some of the previous work in this field will be reviewed briefly. Kleinstein (2) obtained solutions for velocity, temperature, and concentration profiles in the fully developed region of a turbulent, compressible free jet by solving the linearized boundary-layer equations. Pai (3) solved the transformed boundary-layer equations by using a finite-difference technique. Warren (4) calculated the axial variation of velocity and temperature in a compressible jet by using an integral method and obtained the radial variation of velocity in the potential core and fully developed jet from universal profiles. Szablewski (5) developed an analysis which used a similarity parameter and numerical integration of the boundary-layer equations to obtain velocity and temperature profiles in the core region. Other investigators have also treated various aspects of the compressible free jet problem (6, 7). These solutions, however, were all subject to one or more of the following limitations: restriction to flows where initial velocity and temperature profiles could be represented by step functions, restriction to a

John Tomich is with Esso Research Company, Houston, Texas.

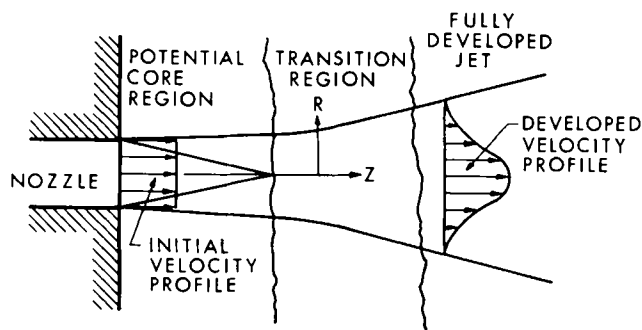


Fig. 1. Structure and nomenclature of a compressible, turbulent, axially symmetric free jet.

turbulent Prandtl number of unity, restriction to the case of a jet exhausting into a moving external stream, and restriction to specific regions of the flow field.

Little experimental data are available on heat and momentum exchange in compressible jets at high subsonic Mach numbers. Corrsin and Uberoi (1) obtained experimental data for elevated temperature, low Mach number flows, while Warren (4) and Snedeker and Donaldson (8) obtained data on jets of subsonic and supersonic speeds at relatively low temperatures.

In the present investigation data have been obtained for round, subsonic turbulent jets of air emerging from cylindrical nozzles ($\frac{1}{4}$ and $\frac{3}{8}$ in. in diameter) into still room temperature air. Initial jet temperatures ranged up to 1,300°F. and Mach numbers ranged from 0.6 to 0.85. The calculational technique uses a variation of a finite-difference technique due to Abbott (9). Solutions are obtained for free jet injection into a medium at rest where initial free jet velocity and temperature profiles are assumed to be step functions. Dynamic eddy transfer coefficients are defined for the turbulent, compressible flow.

Fairly good agreement is obtained between the calculated axial and radial distributions of axial velocity and temperature and the data from this experimental study and those of Corrsin and Uberoi (1). Although the solutions presented in this paper are for one specific physical situation, the same finite-difference technique can be used for the calculation of velocity and temperature fields in jets exhausting into a uniform external stream, jets with initial profiles of velocity and temperature of an arbitrary shape, and jets with variable fluid properties.

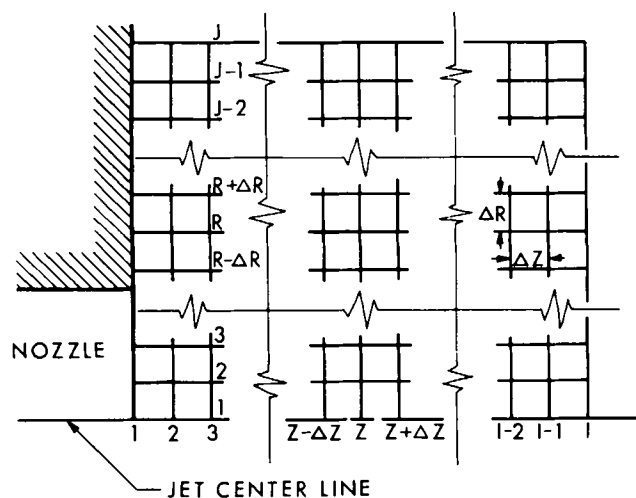


Fig. 2. Schematic diagram of the finite-difference network.

ANALYSIS

A schematic diagram of the free jet showing the coordinate system used is shown in Figure 1. The boundary-layer equations for the conservation of mass, momentum, and energy in the turbulent, compressible, axially symmetric free jet are

$$\frac{\partial}{\partial z} (\rho v_z) + \frac{1}{r} \frac{\partial}{\partial r} (r \rho v_r) = 0 \quad (1)$$

$$\rho v_z \frac{\partial v_z}{\partial z} + \rho v_r \frac{\partial v_z}{\partial r} = \frac{1}{r} \frac{\partial}{\partial r} \left(r \rho \epsilon_v \frac{\partial v_z}{\partial r} \right) \quad (2)$$

$$\rho v_z C_p \frac{\partial t}{\partial z} + \rho v_r C_p \frac{\partial t}{\partial r} = \frac{1}{r} \frac{\partial}{\partial r} \left(r \kappa \frac{\partial t}{\partial r} \right) + \rho \epsilon_v \left(\frac{\partial v_z}{\partial r} \right)^2 \quad (3)$$

The heat capacity and the static pressure are assumed to be constant in these equations. The assumption of constant static pressure has been shown to be a valid assumption for subsonic free jets (7). All densities, velocities, and temperatures have been time smoothed for turbulent flow. The boundary conditions for this free jet flow are

$$\text{At } z = 0 \quad \left. \begin{array}{l} v_z = v_{zj} \\ t = t_j \\ v_r = 0 \end{array} \right\} r < \frac{D}{2}$$

$$\left. \begin{array}{l} v_z = 0 \\ t = t_a \\ v_r = 0 \end{array} \right\} r \geq \frac{D}{2}$$

$$\text{At } r = 0 \quad \left. \begin{array}{l} \frac{\partial v_z}{\partial r} = 0 \\ \frac{\partial t}{\partial r} = 0 \\ v_r = 0 \end{array} \right\} \text{All } z$$

$$\text{As } r \rightarrow \infty \quad \left. \begin{array}{l} v_z \rightarrow 0 \\ t \rightarrow t_a \\ v_r \rightarrow 0 \end{array} \right\} \text{All } z$$

Equations (1) to (3) are now made dimensionless.

$$\frac{\partial}{\partial Z} (P V_z) + \frac{1}{R} \frac{\partial}{\partial R} (R P V_R) = 0 \quad (4)$$

$$P V_z \frac{\partial V_z}{\partial Z} + P V_R \frac{\partial V_z}{\partial R} = \frac{1}{v_{zj} D} \frac{1}{R} \frac{\partial}{\partial R} \left(R P \epsilon_v \frac{\partial V_z}{\partial R} \right) \quad (5)$$

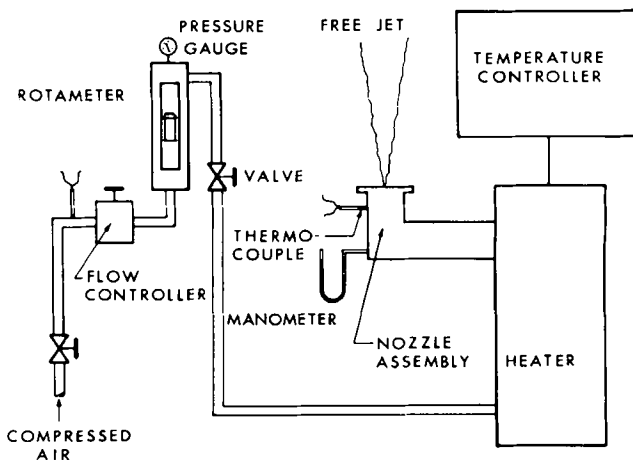


Fig. 3. Schematic sketch of the equipment.

$$PV_Z \frac{\partial T}{\partial Z} + PV_R \frac{\partial T}{\partial R} = \frac{1}{\rho_j v_{zj} D} \frac{1}{R} \frac{\partial}{\partial R} \left(R \frac{\kappa}{C_p} \frac{\partial T}{\partial R} \right) + \frac{v_{zj}}{D(t_j - t_a) C_p} P \epsilon_v \left(\frac{\partial V_Z}{\partial R} \right)^2 \quad (6)$$

The transformed boundary conditions in dimensionless form become

$$\begin{aligned} \text{At } z = 0 \quad & \left. \begin{aligned} V_Z &= 1.0 \\ T &= 1.0 \\ V_R &= 0 \end{aligned} \right\} R < \frac{1}{2} \\ & \left. \begin{aligned} V_Z &= 0 \\ T &= 0 \\ V_R &= 0 \end{aligned} \right\} R \geq \frac{1}{2} \\ \text{At } R = 0 \quad & \left. \begin{aligned} \frac{\partial V_Z}{\partial R} &= 0 \\ \frac{\partial T}{\partial R} &= 0 \\ V_R &= 0 \end{aligned} \right\} \text{All } Z \\ \text{As } R \rightarrow \infty \quad & \left. \begin{aligned} V_Z &\rightarrow 0 \\ T &\rightarrow 0 \\ V_R &\rightarrow 0 \end{aligned} \right\} \text{All } Z \end{aligned}$$

For incompressible jets, expressions for the eddy kinematic viscosity have been obtained semiempirically in terms of parameters of the main jet flow with either Prandtl's constant exchange coefficient, von Karman's hypothesis, or Taylor's vorticity theory (10). Solutions incorporating these expressions have agreed well with experimental data. Therefore the expressions for eddy kinematic viscosity derived with these theories have become generally accepted for the solution of incompressible free jet flows.

For compressible free jet flows, however, the mechanism of the transport phenomena has not been semiempirically determined, and few empirical formulations have resulted in solutions which compare well with experimental data. Kleinstein (2) has stated that a dynamic eddy transfer coefficient $P \epsilon_v$ must be used as a measure of the transport phenomena for compressible flows. Using a semiempirical approach he deduced the following form for this transfer coefficient:

$$P \epsilon_v = 0.0183 P_a^{1/2} v_{zj} \frac{D}{2} \quad (7)$$

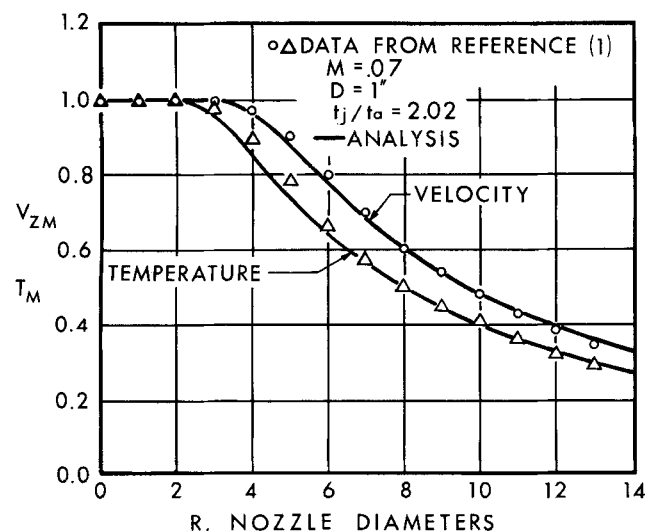


Fig. 4. Comparison of the analysis with experimental data for the axial decay of axial velocity and temperature.

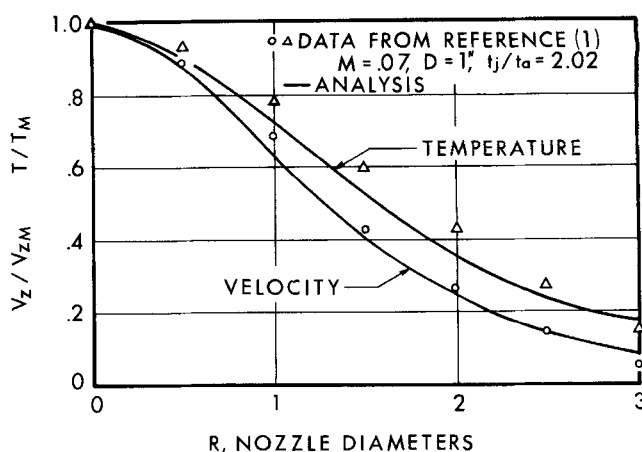


Fig. 5. Comparison of the analysis with experimental data for the radial distribution of axial velocity and temperature at $Z = 15$.

Warren (4), in his analysis of the compressible free jet, proposed two expressions for the eddy kinematic viscosity, one for the potential core region and another for the fully developed jet. These expressions were similar to Prandtl's constant exchange coefficient. Warren found, however, that the experimentally determined constant in Prandtl's constant exchange coefficient was a linear function of the Mach number at the nozzle exit. Warren's momentum transfer coefficients are

Core region:

$$\epsilon_v = (0.0434 - 0.0069M) (r_5 - r_c) \frac{v_{zj}}{2} \quad (8)$$

Fully developed jet:

$$\epsilon_v = (0.0434 - 0.0069M) r_5 \frac{v_{zj}}{2} \quad (9)$$

In the present approach Kleinstein's eddy transfer coefficient has been modified slightly to provide a better correlation with experimental data. The eddy transfer coefficient for momentum is

$$P \epsilon_v = k(M) P_a^{1/2} P_M v_{zj} D f_v(Z) \quad (10)$$

where

$$f_v(Z) = 0.2 \text{ for } Z \leq Z_{cv}$$

$$= 1.0 \text{ for } Z > Z_{cv}$$

$$Z_{cv} = 4.73 P_a^{-1/2}$$

$$k(M) = 0.00972 - 0.00751 M + 0.00298 M^2$$

Also, if the turbulent Prandtl number is only a function of axial position, the eddy thermal conductivity may be expressed as

$$K = k(M) C_p P_a^{1/2} P_M \rho_j v_{zj} D f_T(Z) / N_{Pr} \quad (11)$$

where

$$f_T(Z) = 0.2 \text{ for } Z \leq Z_{cT}$$

$$= 1.0 \text{ for } Z > Z_{cT}$$

$$Z_{cT} = 3.43 P_a^{-1/2}$$

$$N_{Pr, \text{Air}} = 1.0 \text{ for } Z \leq Z_{cT}$$

$$= 0.715 \text{ for } Z > Z_{cT}$$

These transfer coefficients differ from those of Kleinstein's analysis (2) by the addition of P_M , $f_v(Z)$, $f_T(Z)$, and the function of Mach number. Although Kleinstein defined the extent of the core regions for velocity and temperature (Z_{cv} and Z_{cT} , respectively), his transfer coefficients

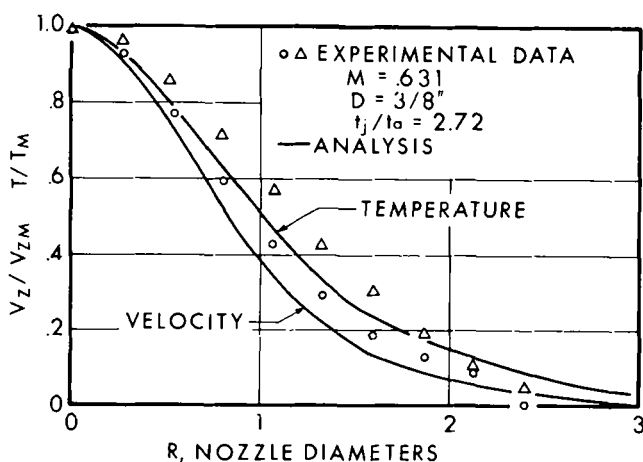


Fig. 6. Comparison of the analysis with experimental data for the axial velocity and temperature.

cients did not apply in the core regions. The addition of the terms $f_v(Z)$ and $f_T(Z)$ serves to define average eddy transport coefficients for the core regions. Note also that the turbulent Prandtl number in the temperature core region is unity, indicating equal turbulent transport rates of momentum and energy. The turbulent Prandtl number for the remainder of the flow field has been found to be roughly constant and very nearly equal to the laminar

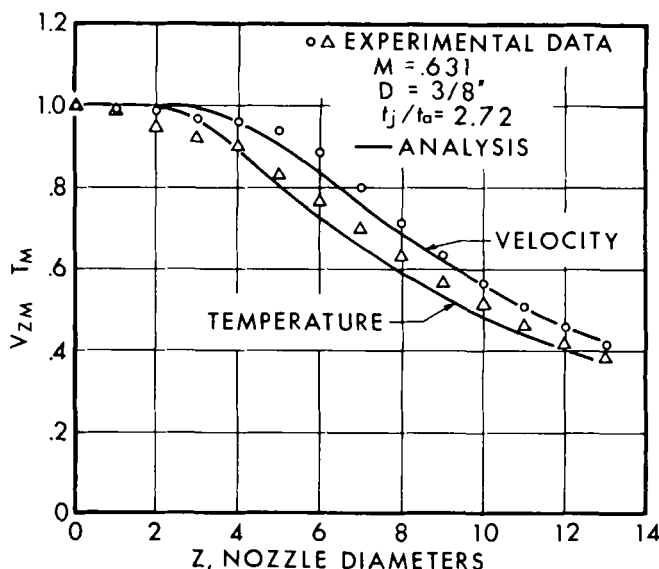


Fig. 7. Comparison of the analysis with experimental data for the radial distribution of axial velocity and temperature at $Z = 11$.

$$\frac{\partial V_z}{\partial R} = \frac{V_z(Z + \Delta Z, R + \Delta R) - V_z(Z + \Delta Z, R - \Delta R)}{2\Delta R} \quad (18)$$

$$\frac{\partial^2 V_z}{\partial R^2} = \frac{V_z(Z + \Delta Z, R + \Delta R) - 2V_z(Z + \Delta Z, R) + V_z(Z + \Delta Z, R - \Delta R)}{\Delta R^2} \quad (19)$$

Prandtl number (1, 2). An analysis of all experimental data of this study and of previous investigations showed that the addition of P_M and the function of Mach number would provide an improved axial variation of the flow properties.

Substituting Equations (10) and (11) into Equations (5) and (6), we have

$$\underline{PV_z} \frac{\partial V_z}{\partial Z} + \underline{PV_R} \frac{\partial V_z}{\partial R} = A_v \frac{1}{R} \frac{\partial}{\partial R} \left(R \frac{\partial V_z}{\partial R} \right) \quad (12)$$

where

$$A_v = \frac{P_{\epsilon_v}}{v_{zj} D} = k(M) P_a^{1/2} P_M f_v(Z) \quad (13)$$

$$\underline{PV_z} \frac{\partial T}{\partial Z} + \underline{PV_R} \frac{\partial T}{\partial R} = A_T \frac{1}{R} \frac{\partial}{\partial R} \left(R \frac{\partial T}{\partial R} \right) + N_{Ec} A_v \left(\frac{\partial V_z}{\partial R} \right)^2 \quad (14)$$

where

$$A_T = \frac{K}{C_p \rho_j v_{zj} D} = k(M) P_a^{1/2} P_M f_T(Z) / N_{Pr} \quad (15)$$

$$N_{Ec} = v_{zj}^2 / C_p (t_j - t_a) \quad (16)$$

The finite-difference solution used here is a variation of the fully implicit method of Abbott (9) for constant-temperature, incompressible, axially symmetric flows. The following finite-difference approximations for derivatives at $(Z + \Delta Z, R)$ were used:

$$\frac{\partial V_z}{\partial Z} = \frac{V_z(Z + \Delta Z, R) - V_z(Z, R)}{\Delta Z} \quad (17)$$

Similar expressions were used for the derivatives of radial velocity, temperature, and density. Another radial derivative form, which is used in the continuity equation in order to make the application of the boundary conditions easier, is

$$\frac{\partial V_R}{\partial R} = \frac{V_R(Z + \Delta Z, R) - V_R(Z + \Delta Z, R - \Delta R)}{\Delta R} \quad (20)$$

The finite-difference approximations were substituted into Equations (4), (12), and (14), which, along with Equations (13), (15), and (16), the equation of state, and the boundary conditions, comprise the system of nonlinear algebraic equations to be solved at each point of the finite-difference network (see Figure 2). Also, it is obvious that some radial position, at which velocities and temperatures are essentially equal to those at an infinite radial distance, must be chosen to represent an infinite radial distance in the numerical calculations. This radial position was determined by the capabilities of an IBM 7072.

The system of algebraic equations was linearized by taking the coefficients [shown as the underlined coefficients in Equations (12) and (14)] of the nonlinear terms at their known value on the previous line of the network, or at Z . The resulting system of simultaneous, linear algebraic equations was solved by using Thomas' method (11) for initial values of V_z , V_R , and T at each point of the line $Z + \Delta Z$. The computational accuracy was then improved with an iterative procedure, and the solution is carried downstream to $Z + 2\Delta Z$, etc. A procedure developed by Wegstein (12) was used to accelerate the iterative process.

Near $Z = 0$ smaller step sizes were required (13) to converge to the correct solution than were required further downstream where the gradients are much smaller. The

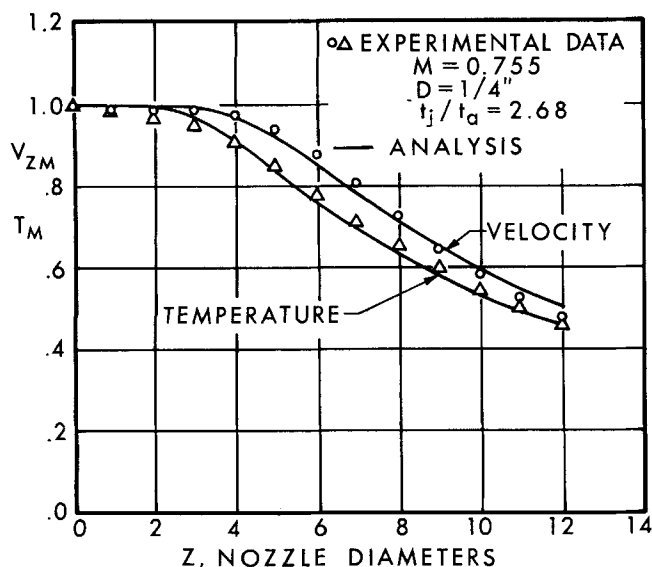


Fig. 8. Comparison of the analysis with experimental data for the axial decay of axial velocity and temperature.

step sizes were increased downstream in order to speed up the numerical solution. The finite-difference network in Figure 2 shows only the section of the finite-difference network containing the smallest step sizes.

EXPERIMENTAL PROCEDURE

A schematic sketch of the equipment, which was built as part of the equipment for the study of impinging jets and was used to gather the free jet data, is shown in Figure 3. The compressible fluid for the free jet was air, which was taken from the tank of an air compressor. The flow rate of the air was controlled by a diaphragm type of flow controller and measured by a metering rotameter. The air flow rate was extremely steady and did not vary noticeably during the course of an experimental run. The air then passed into an electrical resistance heater. The air temperature at the outlet of the heater was controlled by using on-off pyrometer regulation of one of the heater's two electrical circuits. The air then entered the stainless steel nozzle assembly.

The nozzle assembly consisted of a plenum chamber and a circular convergent nozzle with a short constant area throat. The plenum chamber contained three removable sections of fine screening, and the throat of the nozzle was short to provide as uniform velocity and temperature profiles as possible at the nozzle exit. The nozzle assembly was designed to accommodate interchangeable nozzles $\frac{1}{4}$ and $\frac{3}{8}$ in. in diameter. Although the temperature of the air was only controlled at the outlet of the heater, the air temperature at the nozzle, which was as high as $1,300^{\circ}\text{F}$, never varied more than 2°F . The temperature and pressure of the air were measured in the plenum chamber. Also, an annular piece of stainless steel plate was placed in the plane of the nozzle exit to prevent entrainment of ambient air from behind the nozzle; this ensured the assumed condition of a jet exhausting into a medium at rest.

It was desirable to direct the hot air of the jet vertically upward so that the angular symmetry of the circular jet would not be destroyed by natural convection effects and the stability of the jet would be enhanced. Since attempts to align the nozzle before a steady state had been attained resulted in movement of the nozzle during the transient heating period, the nozzle was aligned so that the jet axis was vertical after steady state conditions were reached. In order to do this, the nozzle assembly was attached to a base table by three leveling legs and flexible stainless steel pipe was used between the heater and the nozzle assembly.

All measurements were made at steady state. Two total head pressure probes and one stagnation temperature probe were used to measure velocity and temperature profiles in the

free jet. The total head probe for use in the potential core and transition regions was of standard design and was 0.025 in. in diameter. A Kiel type of total head pressure probe (14) was used in the fully developed jet where the flow direction was not so well known. The miniature stagnation temperature probe was of a standard design and was about 0.060 in. in diameter. It contained a chromel-alumel type of thermocouple.

Stagnation temperature and total pressure traverses were started by aligning telescopically the probe used in the center of the nozzle at the plane of the nozzle exit. With this location as a reference point, the probe could be moved to any position in the free jet flow by using the probe positioning jig, which was constructed from three lathe drive mechanisms and could position the probes within 0.001 in. of the desired location. The probe positioning jig was mounted on leveling legs and could be aligned so that one probe movement was along the axis of the jet.

Measurement of the axial decay of velocity and temperature was made at axial distances up to twelve to fourteen nozzle diameters. Radial traverses were usually made at axial distances of four, eight, and eleven nozzle diameters. Data were taken with both $\frac{1}{4}$ - and $\frac{3}{8}$ -in. diameter nozzles at initial jet Mach numbers from 0.6 to 0.85 and at initial jet temperature ratios (t_j/t_a) from 2.2 to 2.92. Velocity and temperature were calculated from the original data which were taken as total head pressure and stagnation temperature. Transducers were used to measure the total head pressures, while the stagnation temperatures were recorded on a multi-point recording potentiometer.

RESULTS

The results of the numerical calculations are compared with the experimental data of Corrsin and Uberoi (1) in Figures 4 and 5. The jet Mach number (M) and the jet temperature ratio (t_j/t_a or P_a) at which these data were taken were about 0.07 and 2.0, respectively. Figure 4 shows the results of the calculations compared with data for the axial decay of axial velocity and temperature. Calculated radial distributions of axial velocity and temperature at $Z = 15$ are compared with the experimental data of Corrsin and Uberoi in Figure 5.

Calculated results are compared with experimental data from two experimental runs of the present investigation (15) in Figures 6 through 10. A comparison of the calculated axial decay of axial velocity and temperature with data from one experimental run made with a $\frac{3}{8}$ in. diameter nozzle at a jet Mach number and temperature ratio of 0.631 and 2.72, respectively, is shown in Figure 6. Radial distributions of axial velocity and temperature at $Z = 11$ are compared with data from the same experimental run in Figure 7. Data for the decay of axial velocity and tem-

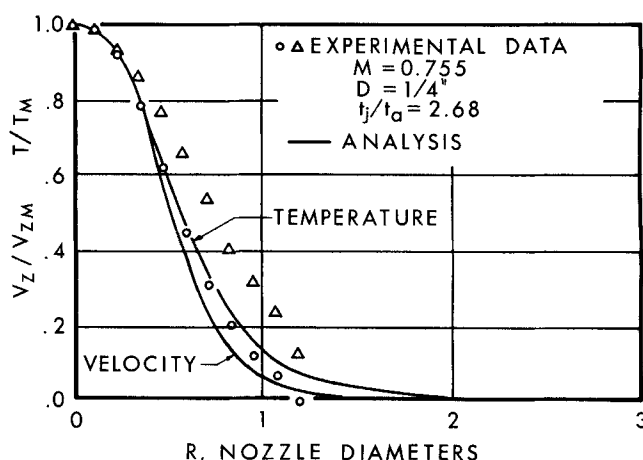


Fig. 9. Comparison of the analysis with experimental data for the radial distribution of axial velocity and temperature at $Z = 4$.

perature from an experimental run made with a 1/4-in. diameter nozzle at a jet Mach number of 0.755 and a jet temperature ratio of 2.68 are compared with the calculated results in Figure 8. Data for the radial variation of axial velocity and temperature are compared with the calculated results at $Z = 4$, which is at the end of the core region and the beginning of the transition region, and at $Z = 11$, which is in the fully developed jets, in Figures 9 and 10.

The effect of the initial free jet Mach number on the axial decay of axial velocity is shown in Figure 11. Although there is a small difference in the initial jet temperature ratios for the two runs for which data is shown here, the effect of this difference is small compared with the effect of the difference in the initial jet Mach numbers. Also, calculated results for the radial distribution of the radial velocity component in the free jet are shown in Figure 12. There were no experimental measurements of radial velocity available for comparison with the calculated results.

DISCUSSION

It is evident that there is good general agreement between the calculated axial velocity and temperature profiles and the experimental results of this and previous investigations. There are some minor deviations between experiment and calculation, especially in the jet transition region. These are probably due to oversimplifications in the forms used for the eddy transfer coefficients.

The calculated radial distributions of velocities in the axial direction and temperatures consistently predict slightly lower velocities and temperatures over most of the radial distribution than are found experimentally. Much larger deviations occur, especially for high Mach numbers flows, if the viscous dissipation term of the energy equation [the last term of Equations (6) and (14)] is not included. At very large radial distances the calculated quantities become higher than the experimentally determined ones, but this deviation is very minor considering the accuracy of the data at positions far from the jet axis.

It is possible that there should be a function of radial position included in the transfer coefficient expressions to improve the agreement between calculated radial distributions and experimental data. However, because of the magnitude of the deviations and the lack of knowledge of the turbulent structure of compressible free jets, it was not deemed justifiable to include such a modification at

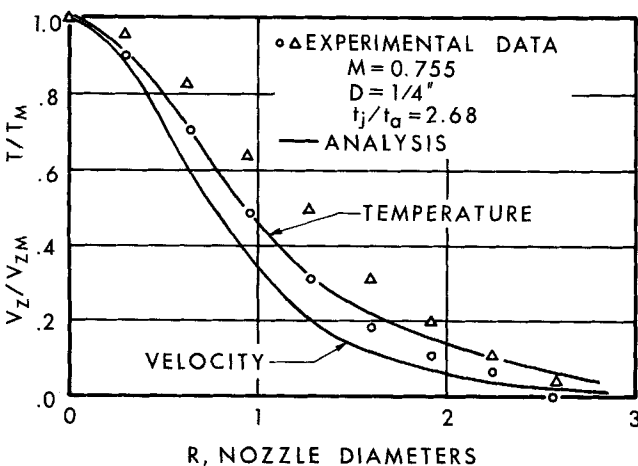


Fig. 10. Comparison of the analysis with experimental data for the radial distribution of axial velocity and temperature at $Z = 11$.

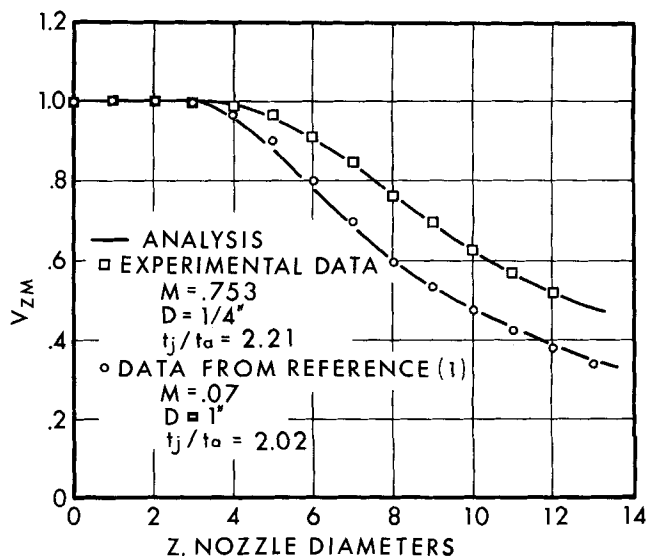


Fig. 11. The effect of initial jet Mach number on the axial decay of axial velocity.

this time. The possibility that the differences in the results occur because the radial position chosen to represent an infinite radial distance in the numerical calculations is not large enough was investigated. Extensive calculations showed that this was not a factor.

The results demonstrate that the specification of only two initial properties suffices to provide the velocity and temperature characteristics of the compressible turbulent free jet. These are the jet Mach number and the jet temperature ratio.

The effects of the jet temperature ratio and jet Mach number on the axial decay of velocity and temperature reported by Warren (4) have been corroborated. That is, for a given jet Mach number, an increase in the jet temperature ratio causes a more rapid decay of velocity and temperature; while for a given jet temperature, an increase in the jet Mach number causes a less rapid decay of the two quantities. The effect of jet Mach number on axial decay is illustrated in Figure 11.

Another advantage of the present calculational method is that calculated results for the radial distribution of the radial velocity component can also be obtained. The positive radial velocity near the jet axis is thought to be caused by the spread of the jet as it moves downstream, while the negative (inward) radial velocity at the larger radial distances is thought to be caused by the entrain-

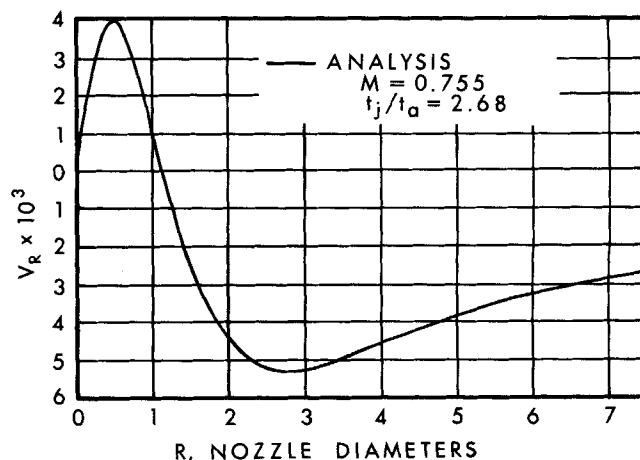


Fig. 12. Calculated radial distribution of radial velocity at $Z = 11$.

ment of ambient air. Experimental measurement of this velocity component will have to await the use of more sensitive techniques such as hot-wire anemometry.

CONCLUSIONS

A finite-difference calculational technique has made possible a fairly simple yet very general solution of the boundary-layer conservation equations for a compressible, turbulent, axially symmetric free jet. The generality of the present solution has eliminated the need for some of the simplifying assumptions that were required in previous investigations in order to obtain a solution. Modifications of eddy transfer coefficients given in the literature result in solutions which agree well with experimental data. However, the finite-difference technique has been set up so that even more complex forms of eddy transfer coefficients can be inserted when the accuracy of the available data justifies it. Another advantage of this calculational method is that distributions of the radial component of velocity are also obtained.

The jet Mach number and the jet temperature ratio are the only two initial jet properties which are necessary to obtain a good description of the compressible turbulent free jet flow in terms of dimensionless variables. The axial velocity and temperature has been found to decay faster when jet Mach numbers are decreased or jet temperature ratios are increased.

The experimental system which has been developed has been found to give repeatable data on the variation of velocity and temperature in a compressible, turbulent, axially symmetric free jet. An experimental program has been carried out, as part of a study of impinging jets, to obtain free jet data at a variety of initial jet conditions where there was a lack of experimental data, namely, at high initial jet temperatures and high subsonic Mach numbers.

ACKNOWLEDGMENT

The authors acknowledge support received from NASA Multi-Disciplinary Research Grant NSG-58 by Washington University for the initiation of the work reported above and from NSF Grant No. 22296 to the Washington University Computational Facilities which made possible the extensive computations required for this study. They would also like to acknowledge the assistance of Fred Epstein of the Industrial Engineering and Equipment Company of St. Louis in the design, fabrication, and testing of the air heater, and the Mechanical and Civil Engineering Departments of Washington University in designing and supplying part of the experimental equipment.

NOTATION

A_v = constant in dimensionless momentum equation, defined by Equation (13)
 A_T = constant in dimensionless energy equation defined by Equation (15)
 C_p = heat capacity at constant pressure
 D = diameter of the jet nozzle
 $f_v(Z)$ = function defining the axial dependence of the eddy momentum transfer coefficient, defined by Equation (10)
 $f_T(Z)$ = function defining the axial dependence of the eddy thermal conductivity, defined by Equation (11)
 I = number of last line of finite-difference network in Z direction
 J = number of last point of finite-difference network in R direction
 $k(M)$ = function defining the Mach number dependence of the eddy momentum transfer coefficient and

the eddy thermal conductivity, defined by Equation (10)

M = initial jet Mach number
 N_{Ec} = Eckert number, defined by Equation (16)
 N_{Pr} = turbulent Prandtl number, $C_p \rho \epsilon_v / \kappa$
 r = radial coordinate
 r_5 = radial coordinate at point in jet where $v_z/v_{zM} = 0.5$
 r_c = radial coordinate of inner boundary of potential core for velocity
 R = dimensionless radial coordinate, r/D
 t = temperature
 T = dimensionless temperature, $(t - t_a)/(t_j - t_a)$
 v_r = radial velocity
 V_R = dimensionless radial velocity, v_r/v_{zj}
 v_z = axial velocity
 V_Z = dimensionless axial velocity, v_z/v_{zj}
 z = axial coordinate
 Z = dimensional axial coordinate, z/D

Greek Letters

ΔZ = finite-difference step size in axial direction
 ΔR = finite-difference step size in radial direction
 ϵ_v = eddy kinematic viscosity
 κ = eddy thermal conductivity
 ρ = density
 P = dimensionless density, ρ/ρ_j

Subscripts

a = properties of ambient receiving medium
 cv = potential core for velocity
 ct = potential core for temperature
 i = initial properties of jet
 M = property on jet axis
 T = energy equation
 v = momentum equation
 r, R = radial component
 z, Z = axial component
 5 = properties at the point in the jet where $v_z/v_{zM} = 0.5$

LITERATURE CITED

- Corrsin, Stanley, and M. S. Uberoi, *Natl. Advisory Comm. Aeronaut. Tech. Note 1865* (1949).
- Kleinstein, G., *J. Spacecraft Rockets*, **1**, 403 (1964).
- Pai, S. I., *Quart. Appl. Math.*, **10**, 141 (1952).
- Warren, W. R., Ph.D. thesis, Princeton Univ., N. J. (1957).
- Szablewski, W., *Intern. J. Heat Mass Transfer*, **6**, 739 (1963).
- Cohen, N. S., *Rept. TM 1 SRO*, Aerojet-General Corp., Sacramento, Calif. (1964).
- Abramovich, G. N., "Turbulent Jets Theory," pp. 8, 278-316, Armed Services Tech. Information Agency, Translation AD 283858 (1962).
- Snedeker, R. S., and C. duP. Donaldson, *Rept. AD 461622*, Defense Documentation Center for Scientific and Technical Information, Cameron Station, Alexandria, Va.
- Abbott, M. R., *Computer J.*, **7**, 47 (1964).
- Schlichting, Hermann, "Boundary Layer Theory," pp. 590-609, McGraw-Hill, New York (1955).
- Lapidus, Leon, "Digital Computation for Chemical Engineers," pp. 254-255, McGraw-Hill, New York (1962).
- Wegstein, J. H., *Commun. Assoc. Computing Mach.*, **1**, 9 (1958).
- Hwang, C. L. and L. T. Fan, *Appl. Sci. Res.*, **A13**, 401 (1965).
- Kiel, G., *Natl. Advisory Comm. Aeronaut. Tech. Memo TM 775* (1935).
- Tomich, J. F., D.Sc. dissertation, Washington Univ., St. Louis, Mo. (1967).

Manuscript received September 21, 1966; revision received February 9, 1967; paper accepted February 10, 1967.